Journal of Solid State Chemistry 182 (2009) 3207–3210

Contents lists available at ScienceDirect

Journal of Solid State Chemistry

journal homepage: www.elsevier.com/locate/jssc

Rapid Communication

Density functional study on electronic and optical properties of C (or N)-doped cubic cerium dioxide

Yufen Zhang [a,*], Xian Zhao [b]

[a] Department of Chemistry and Chemical Technology, Jinan University, Jinan 250022, PR China
[b] State Key Lab of Crystal Materials, Shandong University, Jinan 250100, PR China

ARTICLE INFO

Article history:
Received 14 July 2009
Received in revised form
12 August 2009
Accepted 14 August 2009
Available online 20 August 2009

Keywords:
DFT
Electronic and optical properties
Doping of C (or N)
CeO_2

ABSTRACT

Density functional calculations were performed on electronic and optical properties of C (or N)-doped cubic cerium dioxide (CeO_2). When O is replaced by C (or N) in CeO_2, obvious band-gap (E_g) reduction is observed. Meanwhile, it is interesting to find that the substitutional doping of C (or N) in CeO_2 obviously increases the O 2*p*–Ce 4*f* transition intensity and also the refractive index. The increase in the O 2*p*–Ce 4*f* transition intensity on going from undoped, N-doped and C-doped CeO_2 was related to the covalent character of the Ce–O bond. Compared with the undoped CeO_2, the C (or N)-doped CeO_2, with steep absorption peaks at lower energy, can be used for visible-light absorption applications.

1. Introduction

Lanthanide dioxides (LnO_2) with a cubic fluorite structure have attracted much attention for their wide applications as optical component materials and laser hosts. Out of LnO_2 type compounds, cubic fluorite ($Fm3m$) cerium dioxide (CeO_2) is well known for the broad applications in automobile exhaust catalysts as oxygen storage, due to its ability to take up and release oxygen under oxidizing and reducing conditions. With a band gap of 3.2 eV and a high UV absorption and a refractive index of 2.35, cubic CeO_2 has been proposed as a potential substitute for TiO_2 and its optical properties has been the focus of intensive research [1–9] for recent years. It has been reported that substitutional doping of N (or C) in TiO_2 has a profound effect on the electronic and optical properties [10–13]. So it can be speculated that incorporation of low concentrations of N or C impurity in cubic CeO_2 could induce a different electronic structure and optical properties that may lead to new applications. It is therefore timely to investigate the electronic structure of these systems. For recent years, CeO_2 based materials have attracted many experimental and theoretical investigations [9,14–19], in which, the method of density functional theory (DFT) has been successfully used in predicting crystal structures and properties of CeO_2 [9,14–16]. In this paper, we carried out first-principles calculations based on DFT to investigate the electronic structures of the C (or N)-doped cubic CeO_2 (denoted CeO_2:C or N) and probed the role of anion 2*p* and Ce 4*f* orbitals in the optical properties, including the optical gap, O 2*p*–Ce 4*f* transition intensity and the refractive index. We focus our attention on the trends in the electronic and optical properties of C-doped, N-doped and undoped CeO_2. We hope that such calculations could provide more insights into the relation between the structure and the properties for CeO_2.

2. Computational method and details

The first-principles electronic structure calculations based on DFT [20] within CASTEP 4.1 code [21] were carried out to determine the stability and electronic structures of the undoped and C (or N) doped CeO_2. The Vanderbilt ultrasoft pseudopotential [22] with generalized gradient approximation due to Perdew Burke Ernzerhof (GGA-PBE) [23] for exchange-correlation effects was used to model our systems. A cutoff energy of 410 eV for C (or N) doped and undoped CeO_2 in the plane wave expansion was employed in the calculations. A $4\times4\times4$ Monkhorst–Pack grid [24] was used for integration over the irreducible part of the Brillouin zone of the doped and undoped CeO_2. Good convergence was achieved with the cutoff energy and number of *k* points. The default convergence criteria of CASTEP was applied within energy tolerance 5.0e–6 eV/atom, max force tolerance 0.01 eV/Å, max displacement tolerance 5.0e–4 Å and max stress tolerance 0.02 GPa. To explore the electronic and optical properties of these solid solutions, we employed a 96-atoms supercell (containing $2\times2\times2$ full cubic cells) with the starting configuration of cubic CeO_2 suggested in Ref. [15]. We substituted O atoms by C (or N)

* Corresponding author.
E-mail address: yufen720924@126.com (Y. Zhang).

0022-4596/$ - see front matter © 2009 Elsevier Inc. All rights reserved.
doi:10.1016/j.jssc.2009.08.017

atoms to model substitutional C or N neutral impurity in CeO_2, the resulting supercells are $Ce_{32}O_{60}C_4$ and $Ce_{32}O_{60}N_4$. Within the Broyden–Fletcher–Goldfarb–Shanno (BFGS) scheme [25], geometry optimization was performed under *Fm*3*m* space group allowing both cell parameter and internal coordinates relaxation. In the electronic and optical property calculation, the underestimation of the band gap (inherent in DFT calculations) was corrected by introducing a "scissors operator" (0.9 eV), by which the conduction band positions were raised in energy prior to the interband transition strength calculation to match the general features of the measured imaginary part of dielectric function [9].

3. Results and discussions

3.1. Structural stability and population analysis

The calculated equilibrium structural parameters and the results of population analysis of three structures are summarized in Table 1. The calculated equilibrium structural parameter *a* for CeO_2 is 5.464 Å, which is in good agreement with the experimental value of 5.416 Å [26]. This can demonstrate the applicability of our theoretical model in geometry optimization for CeO_2. For CeO_2:C (or N), the equilibrium structural parameters *a* is ~5% (or 2%) larger than CeO_2.

From the results of population analysis, it is clear to find that substitutional doping of C (or N) will not change the Mulliken charge of O atoms, but obviously lower the charge of Ce atoms, because C (or N) is more likely to donate electron to Ce than O atoms. The bond order between a pair of atoms is a measure of the strength of the bond. It can be calculated from the overlap integrals between the Bloch functions with an atomic basis expansion [27]. The total bond order of a crystal can be obtained by multiplying the individual bond order by the number of bonds per molecular unit. In Table 1, it is interesting to find that the Mulliken bond order for Ce–C is ~0.16 (bond length = 2.434 Å) obviously decrease, for Ce–N ~0.23 (2.396 Å) slightly increase than Ce–O ~0.21 (2.366 Å), and the total bond order both for C-doped (6.74) and for N-doped CeO_2 (6.92) obviously increase, compared with undoped system (6.72). The amazing part is that in going from CeO_2:C (or N) to CeO_2, the total 30 Ce–O bond order are actually increased by ~1.9 (or ~2.5)%. So it can be predicted that CeO_2:C (or N) is much more covalent than CeO_2.

3.2. Electronic properties

Fig. 1 shows the calculated density of states (DOS) of the C-doped, N-doped and undoped CeO_2 96-atoms supercell. In

Table 1
Calculated equilibrium structural parameters and the results of population analysis of three structures.

Structure	*a* (in Å)	Charge (e)	Bond order (bond length, in Å)
c-CeO_2	5.464	O: −0.65 Ce: 1.30	Ce–O: 0.21 (2.366) In total: 6.72 In total of In total of 30 Ce–O: 6.30
c-CeO_2:C	5.495	C: −0.48 O: −0.65 Ce: 1.26; 1.29	Ce–C: 0.16 (2.434) In total: 6.74 In total of 30 Ce–O: 6.42
c-CeO_2:N	5.476	N: −0.61 O: −0.65 Ce: 1.28; 1.29	Ce–N: 0.23 (2.396) In total: 6.92 In total of 30 Ce–O: 6.46

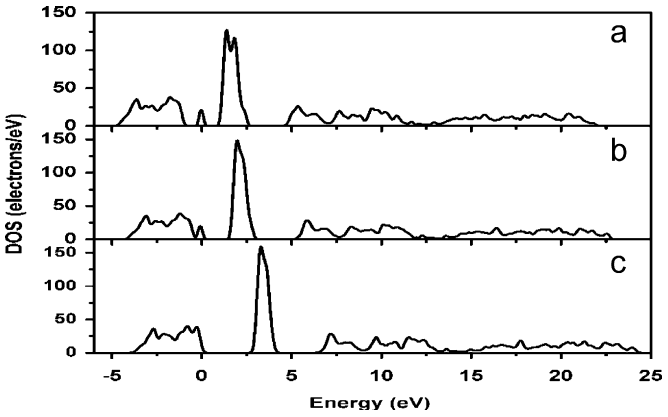

Fig. 1. DOS of (a) C-doped; (b) N-doped and (c) undoped CeO_2.

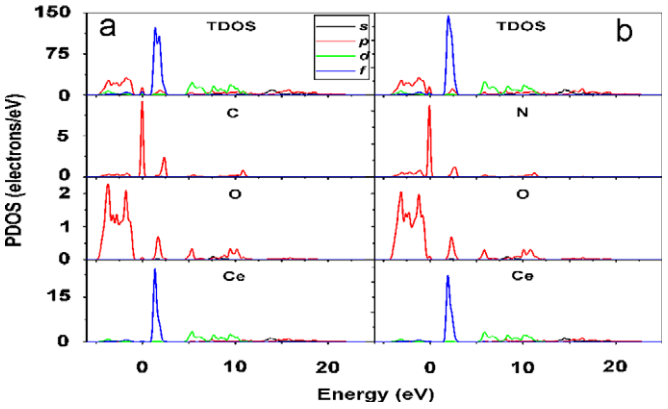

Fig. 2. PDOS of (a) C-doped and (b) N-doped CeO_2.

Fig. 2, we plot the total DOS (TDOS) and partial DOS (PDOS) spectra of both C-doped and N-doped structures. In Figs. 1 and 2, the Fermi energy (E_f) locates at ~0 eV for both undoped and N-doped CeO_2, for C-doped CeO_2 $E_f = \sim -0.9$ eV. For the doped systems, the C (or N) concentration is 6.25%, which results from substituting four O atoms with four C (or N) atoms in a 96-atoms supercell. There is only one anion site in *c*-CeO_2, so substituting O atom with C (or N) needs not consider the site preference. When O is replaced by C (or N) in CeO_2, a bandgap (E_g) reduction is observed. For CeO_2:C (Fig. 1a), an impurity band is clearly found in the band gap. In the case of CeO_2:N (Fig. 1b), an obvious increase at the top of valence band makes the width of valence band broaden.

From the result of Figs. 1 and 2, it is found that the valence band is mainly composed of O 2*p* orbitals and the conduction band of mainly from the contribution of Ce 5*d* orbitals is located at 5.38, 4.91 and 6.18 eV, above the valence band for C-doped, N-doped and undoped CeO_2, respectively. Between valence band and conduction band, the Ce 4*f*-block band is located at 1.73, 1.21 and 2.45 eV, above the top of the O 2*p*-block bands in C-doped, N-doped and undoped CeO_2. For C-doped system (Fig. 2a), the impurity band in the band gap originates from the C 2*p* orbitals, which are the only state mainly located at the impurity band. In Fig. 2b, the increase of TDOS at the top of valence band for CeO_2:N is introduced by the N impurity, because the N 2*p* orbitals are the only states mainly located at the valence band maximum.

The width of valence band varies from 4.0 to 4.5 to 4.1 eV on going from C-doped, N-doped and undoped CeO_2. The valence band is higher in energy for C-doped CeO_2, but lower for N-doped

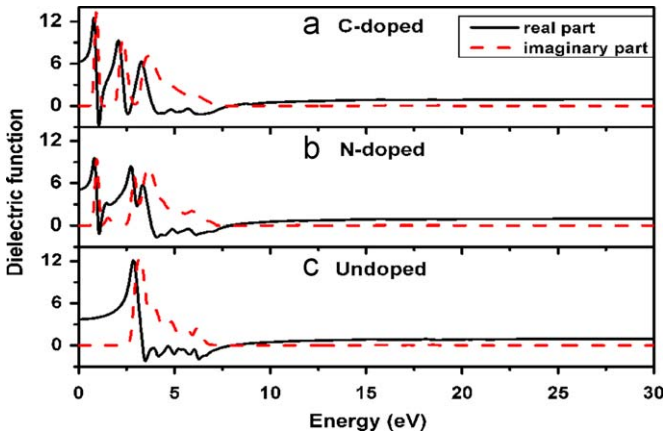

Fig. 3. Real and imaginary part of dielectric functions of three structures.

CeO_2 than for undoped CeO_2. The bottom of conduction band is higher in energy for both C-doped and N-doped CeO_2 than for undoped CeO_2. The width of the Ce 4*f*-block band increases from 1.2 to 1.4 to 1.5 eV on going from undoped, N-doped and C-doped systems. The position of the Ce 4*f*-block band obviously shifts to lower energy for both C-doped and N-doped CeO_2. These may reflect the stronger mixing between Ce 4*f*–C (or N) 2*p* than Ce 4*f*–O 2*p* orbitals, which may be the reason to cause the O 2*p*–Ce 4*f* gap and also the band gap reduction. Fig. 2 clearly shows a substantial obvious mixing between Ce 4*f* and anion 2*p* orbitals.

3.3. Dielectric constants

The optical properties of C-doped, N-doped and undoped CeO_2 were also calculated. For all the three systems, the calculated dielectric functions, including the real part ε_1 and imaginary part ε_2, were calculated up to 30 eV and shown in Fig. 3.

The static dielectric constant $\varepsilon(0)$ is obtained as the zero frequency limit of the real part of the frequency-dependent dielectric function. The calculated $\varepsilon(0)$ is 3.74 for undoped, 5.11 for N-doped and 6.28 for C-doped CeO_2. Both C-doped and N-doped CeO_2 are larger than undoped system. A larger $\varepsilon(0)$ means a larger refractive index [27]. From a chemical point of view, the refractive index of a compound is a measure of its polarizability [9]. The C (or N)-doped CeO_2 are more covalent than the undoped system, so the overall covalent character is stronger in C (or N)-doped systems than in undoped system. Thus, the polarizability and hence the refractive index should be higher in C (or N)-doped systems. A higher optical density for the C (or N)-doped CeO_2 may have special applications in certain optical components.

In Fig. 3c, the ε_2 plot for undoped CeO_2 exhibits one major absorption peak at 3.17 eV, which is associated with the O 2*p*–Ce 4*f* transition [9]. For C-doped system (Fig. 3a), the ε_2 plot exhibits three major absorption peaks at 0.9, 2.3 and 3.6 eV, respectively. In Fig. 3b, the ε_2 plot for N-doped system also exhibits three major absorption peaks at 0.9, 2.9 and 3.7 eV, respectively. It is clear that the dielectric functions of C (or N)-doped CeO_2 are quite different from those of the undoped system. The splitting of the absorption peak in C (or N)-doped CeO_2 should be attributed to the effect of the impurity band introduced by C (or N) atoms. From the results of Fig. 3, it can be found that CeO_2 present a proper absorption edge for an UV absorber and can be used for UV absorption applications, with a steep absorption peak at the absorption edge ~3.2 eV, which is in good agreement with the results of Goubin et al. [9]. The C (or N)-doped CeO_2, with steep absorption peaks at lower energy region ~0.9–2.9 eV, can be used for visible-light absorption applications.

From the ε_2 curves of C (or N)-doped CeO_2, it is also clear that the absorption intensity associated with the O 2*p*–Ce 4*f* transition increases on going from undoped, N-doped and C-doped CeO_2. Compared with undoped *c*-CeO_2, the C (or N)-doped system has more extended major absorption region. These observations can be understood by comparing the Ce 4*f* surroundings. Each Ce atom is surrounded by eight O atoms in *c*-CeO_2. The O 2*p*–Ce 4*f* transition is associated essentially with the electron excitation from the 2*p* orbitals of eight Ce-connected O atoms to the Ce 4*f* orbitals. Due to the increasing donating electrons ability on going from O, N and C atoms, the O 2*p*–Ce 4*f* transition intensity should increase on going from undoped, N-doped and C-doped systems. This can be explained by the increasing covalent character of the Ce–O bond on going from undoped and C (N)-doped CeO_2 with increasing total bond order (presented in Table 1).

In summary, by first-principles pseudopotential calculations, it is predicted that the substitutional doping of C (or N) in cubic CeO_2 lowers the E_g and also O 2*p*–Ce 4*f* gap, and increases the O 2*p*–Ce 4*f* transition intensity and also the refractive index. The optical gap is associated with the O 2*p*–Ce 4*f* excitation and is influenced by the local environments of Ce atom. An increase in the covalent character of the C (or N)-doped CeO_2 lowers the O 2*p*–Ce 4*f* excitation gap. The increase in the O 2*p*–Ce 4*f* transition intensity on going from undoped, N-doped and C-doped CeO_2 was related to the covalent character of the Ce–O bond. Compared with undoped CeO_2, the C (or N)-doped CeO_2, with steep absorption peaks at lower energy, can be used for visible-light absorption applications.

Acknowledgments

This work was supported by the National Natural Science Foundation of China (NSFC, no. 20473046), Research Program of Ministry of science and Technology (2005CCA00900).

Reference

[1] T. Yamamoto, H. Momida, T. Hamada, T. Uda, T. Ohno, Thin Solid Films 486 (2005) 136.
[2] M. Marabelli, P. Wachter, Phys. Rev. B 36 (1987) 1238.
[3] S. Guo, H. Arwin, S.N. Jacobsen, K. Järrendahl, U. Helmersson, J. Appl. Phys. 77 (1995) 5369.
[4] M. Niwano, S. Sato, T. Koide, T. Shidara, A. Fujimori, H. Fukutani, S. Shin, M. Ishigame, J. Phys. Soc. Jpn. 57 (1988) 1489.
[5] M. Veszelei, L. Kullman, C.G. Granqvist, N. Rottkay, M. Rubin, Appl. Opt. 37 (1998) 5993.
[6] M. Miyauchi, A. Nakajima, T. Watanabe, K. Hashimoto, Chem. Mater. 14 (2002) 2812–2816.
[7] M. Primet, E. Garbowski, in: A. Trovarelli (Ed.), Catalysts by Ceria and Related Materials, Imperial College Press, London, 2002, p. 407.
[8] S. Yabe, M. Yamashita, M. Shigeyosi, T. Kazuyuki, S. Yoshida, R. Li, T. Sato, Int. J. Inorg. Mater. 3 (2001) 1003–1008.
[9] F. Goubin, X. Rocquefelte, M.-H. Whangbo, Y. Montardi, R. Brec, S. Jobic, Chem. Mater. 16 (2004) 662–669.
[10] R. Asahi, T. Morikawa, T. Ohwaki, K. Aoki, Y. Taga, Science 293 (2001) 269–271.
[11] S.U.M. Khan, M. Al-Shahry, W.B. Ingler Jr., Science 297 (2002) 2243–2245.
[12] J. Graciani, Y. Ortega, J.F. Sanz, Chem. Mater. 21 (2009) 1431–1438.
[13] A. Enrique, R. Garcia, Y. Sun, K.R. Reyes-Gil, D. Raftery, Solid State Nucl. Magn. Reson. 35 (2009) 74–81.
[14] N.V. Skorodumova, R. Ahuja, S.I. Simak, I.A. Abrikosov, B. Johansson, B.I. Lundqvist, Phys. Rev. B 64 (2001) 115108.
[15] S. Mehrotra, P. Sharma, M. Rajagopalan, A.K. Bandyopadhyay, Solid State Commun. 140 (2006) 313–317.
[16] S. Fabris, S. de Gironcoli, S. Baroni, G. Vicario, G. Balducci, Phys. Rev. B 71 (2005) 041102.
[17] E. Voloshina, B. Paulus, J. Chem. Phys. 124 (2005) 234711.
[18] C.J. Mao, Y.X. Zhao, X.F. Qiu, J.J. Zhu, C. Burda, Phys. Chem. Chem. Phys. 10 (2008) 5633–5638.
[19] S.D. Carolis, J.L. Pascual, L.G.M. Pettersson, M. Baudin, M. Wo′jcik, K. Hermansson, A.E.C. Palmqvist, M. Muhammed, J. Phys. Chem. B 103 (1999) 7627–7636.
[20] W. Kohn, L.J. Sham, Phys. Rev. 140 (1965) A1133.

[21] M.C. Payne, M.P. Teter, D.C. Allan, T.A. Arias, J.D. Joannopoulos, Rev. Mod. Phys. 64 (1992) 1045.
[22] D. Vanderbilt, Phys. Rev. B 41 (1990) 7892.
[23] J.P. Perdew, K. Burke, M. Ernzerhof, Phys. Rev. Lett. 77 (1996) 3865–3868.
[24] H.J. Monkhorst, J.D. Pack, Phys. Rev. B 13 (1976) 5188.
[25] E. Polak, Computational Methods in Optimization, Academic, New York, 1971, p. 56.
[26] S.J. Duclos, Y.K. Vohra, A.L. Ruoff, A. Jayaraman, G.P. Espinosa, Phys. Rev. B 38 (1988) 7755.
[27] S.-D. Mo, L. Ouyang, W.Y. Ching, I. Tanaka, Y. Komyama, R. Riedel, Phys. Rev. Lett. 83 (1999) 5046.